I&EC research
Industrial & Engineering Chemistry Research
pubs.acs.org/IECR
Article

Catalytic Esterification Using Solid Acid Carbon Catalysts Synthesized by Sustainable Hydrothermal and Plasma Sulfonation Techniques

Sarada Sripada and James R. Kastner*

Cite This: *Ind. Eng. Chem. Res.* 2022, 61, 3928−3940
Read Online
ACCESS | Metrics & More | Article Recommendations | Supporting Information

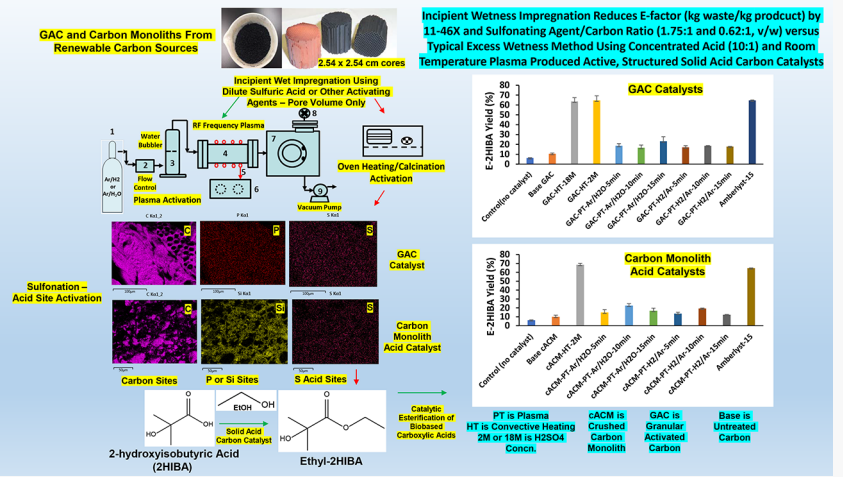

ABSTRACT: Solid acid carbon catalysts were synthesized from wood activated carbon in granular (GAC) and monolith (ACM) forms using incipient wetness and plasma or hydrothermal methods at sulfonation agent:carbon ratios of 0.62:1 to 1.75:1 [v/w, mL/g], significantly lower than a commonly used ratio of 10:1 (6−16× lower). Yet, esterification rates and yields were comparable to those of catalysts generated with excess concentrated sulfuric acid and commercial acid resins. Acid sites were confirmed by multiple methods, and catalytic activity was investigated by batch esterification of 2-hydroxyisobutyric acid. Hydrothermally sulfonated GAC and ACM generated reaction rates and ester yields comparable to commercial Amberlyst-15 (150 °C, 1 h). Room temperature plasma (Ar/H_2O vapor, 10−15 min) successfully sulfonated GAC and ACM but generated lower ester yields, due to lower acid site density. Reaction and reuse studies suggest the hydrothermal incipient wetness and plasma sulfonation methods can sustainably generate solid acid carbon catalysts from renewable biomass for catalytic upgrading biobased organic acids.

1. INTRODUCTION

Homogeneous acids, such as H_2SO_4, have been widely employed for industrial esterification reactions, yet have several limitations including equipment corrosion, lack of reuse, and required treatment of spent effluent.[1] Heterogeneous solid acid catalysts facilitate product separation, ensure catalyst recyclability, and generate little waste, circumventing the environmental impacts associated with their homogeneous counterparts.[2] Solid acids used in esterification reactions include metal oxides, heteropoly acids, zeolites, and acidic ion exchange resins such as Amberlyst-15.[3] Their drawbacks include low porosity and surface area, low acid site density in some materials, poor stability, low water tolerance, and high preparation cost.[4] Although acid resins (e.g., Amberlyst-15) have been employed for catalytic esterification, they can be limited by low thermal stability and are synthesized from petroleum resources.[5] Sulfonated carbon catalysts have received much attention as esterification catalysts because they have Bronsted acid sites,[6] large surface area, are stable under acidic and basic conditions, and can be prepared from renewable lignocellulosics. Carbon supported catalysts are also stable in aqueous environments, which is a prerequisite for equilibrium-limiting esterification reactions that generate water.[7]

Received: January 7, 2022
Revised: February 22, 2022
Accepted: March 3, 2022
Published: March 10, 2022

https://doi.org/10.1021/acs.iecr.2c00086
Ind. Eng. Chem. Res. 2022, 61, 3928−3940

In conventional postgrafting methods (after pyrolysis and activation), sulfonated carbons are typically synthesized by wet impregnation of concentrated or fuming sulfuric acid at elevated temperatures (100−200 °C) for long durations (10−24 h). For instance, activated carbon has been sulfonated using concentrated sulfuric acid (20 mL H_2SO_4/g catalyst) at 150 °C for 16 h.[8] Similarly, carbon fibers have been refluxed in concentrated H_2SO_4 (50 mL H_2SO_4/g catalyst) for 12 h at 150 °C.[9] A review of the postgrafting literature indicates sulfonation agent to carbon ratios (v/w, mL/g) from 7:1 to 50:1, with 10:1 suggested as optimum, and increasing the temperature to 250 °C was shown to increase acid site density in activated carbon.[10,11] These techniques utilize large quantities of acid, necessitating a more environmentally friendly preparation method for scale-up. Modifications to existing hydrothermal methods are essential to minimize activating agent consumption, reduce acidic waste, and ensure optimal sulfonation conditions.

Sustainable strategies for catalyst fabrication have led to the emergence of plasma technology as a design tool for surface modification.[12] Nonthermal plasma (NTP), characterized by a thermodynamic nonequilibrium, permits catalyst synthesis in shorter durations, does not affect the bulk structure, and limits the use of hazardous reagents, thereby minimizing waste.[13] This makes NTP an attractive alternative to the conventional high temperature, longer treatment duration hydrothermal methods. Recently, plasma sulfonation of carbon black (ambient air and N_2/Ar) in dilute sulfuric acid was reported (0.1−1 M, 30 min) resulting in a solid acid catalyst active for decrystallized cellulose hydrolysis.[14,15] Plasma treatment was performed in solution with powdered carbon, using carrier gases such as air, N_2, and argon. Although effective in sulfonating the catalyst surface, continuous generation of plasma in a liquid requires large electrical power compared to vacuum or atmospheric pressure, which increases thermal load on the electrodes and deterioration of the electrode surface.[16] Further, large volumes of dilute acid solution are required for catalyst preparation, reducing process scale-up viability, and the process does not seem applicable to structured carbon. Alternatively, we propose the catalyst can be pretreated with dilute sulfuric acid and subjected to plasma treatment under a vacuum, with hydrogen radical generating carrier gas mixtures such as hydrogen−argon or argon−water vapor. Such a method could be applied to structured catalysts (e.g., pellets and monoliths) used in continuous processing. Activated carbon monoliths combine the advantages of activated carbon and monolithic structure into a single catalyst,[17] because they have high external surface area and interfacial mass transfer rates, and low pressure drop, which facilitates continuous processing. Studies pertaining to activated carbon monoliths as acid catalysts have been scarce.[18]

Esters of hydroxyacids have valuable industrial and medical applications.[19] Eastman Chemical developed an organic cleaning solvent butyl 3-hydroxybutyrate, marketed under the trade name Omnia, by esterifying a diketene with butanol and hydrogenation.[20] Recently, highly cross-linked strong acid resins have been used to directly esterify 3-hydroxybutyric acid (3-HBA) for butyl 3-HBA synthesis (91% conversion, 2 h, 70 °C).[21] 2-Hydroxyisobutyric acid (2-HIBA) is gaining significance as a platform chemical[22] and has been identified as a building block for polymer synthesis. The methyl ester of 2-HIBA is produced from 2-hydroxyisobutyramide and methyl formate, and used for electronic materials, ink cleaning, and an intermediate for agrochemicals and medicine.[23] Ethyl 2-hydroxyisobutyrate (E-2HIBA), which has applications as a solvent for nitrocellulose and cellulose acetate, pharmaceuticals, and organic synthesis, has been less explored.[24] Fermentative production of 2-HIBA has been reported from several recombinant microbial strains,[25] and ethanol is a renewable, biobased platform chemical. Developing a stable solid acid catalyst for 2-HIBA esterification with ethanol would create sustainable avenues for renewable 2-HIBA in fine chemical synthesis and catalytic upgrading of other biobased organic acids.

To reduce the sulfonating agent to carbon ratio, reduce contact time, and lower energy inputs, novel, modified hydrothermal and plasma sulfonation methods were developed. Hydrothermal and plasma sulfonation methods employed the rarely used incipient wetness impregnation (GAC) and sonication (ACM) of wood-based activated carbons using dilute H_2SO_4 (2 M) as the sulfonating agent. This is one of the first reports on the hydrothermal synthesis of sulfonated carbon (GAC) through incipient wetness impregnation with dilute H_2SO_4 and plasma sulfonation by introducing water vapor or hydrogen into a low-pressure plasma reactor. Carrier gases of argon/water vapor and 3% hydrogen/argon were used for plasma treatment. Catalytic efficiency of the hydrothermal and plasma sulfonated GAC and ACM catalysts was assessed in the esterification of 2-HIBA with ethanol as a model reaction and compared to a benchmark catalyst, Amberlyst-15. Our objectives were to develop more sustainable and reusable esterification catalysts from activated carbon, investigate the possibility of modifying the current hydrothermal methods, as well as replacing the hydrothermal steps by plasma methods.

2. MATERIALS AND METHODS

2.1. Chemicals. 2-Hydroxyisobutyric acid ($C_4H_8O_3$, purity >98%) and ethyl 2-hydroxyisobutyrate ($C_6H_{12}O_3$, purity >98%) were purchased from TCI chemicals. Two hundred proof ethanol (purity >99.5%) was procured from Sigma-Aldrich. Sulfuric acid used for carbon sulfonation was purchased from J.T. Baker. Amberlyst-15 (hydrogen form) was obtained from Sigma-Aldrich.

2.2. Specifications of Activated Carbon Materials. A granular activated carbon (Nuchar WV-B 20 GAC) was obtained from Ingevity and used to synthesize the sulfonated carbon catalysts.[7] Nuchar WV-B 20 has a surface area of 1490 m^2/g (Brunauer−Emmett−Teller, BET), pore diameter of 26.9 Å, pore volume of 1.23 cc/g (Barrett−Joyner−Halenda, BJH) and particle size of $1 < d_p < 3$ mm. The wood-based activated carbon monolith (ACM 101-H) was provided by Applied Catalysts (Laurens, SC) and manufactured by coextrusion of 50% activated carbon and 50% of a ceramic binder. Each monolith core has a diameter and length of 1 in. (2.54 cm), 400 cells/in^2 (62 cells/cm^2), wall thickness of 0.01 in. (0.254 mm), cell spacing of 0.0435 in. (1.105 mm), geometric surface area of 70.8 in^2/in^3 (27.88 cm^2/cm^3), open frontal area of 0.593 in^2 (3.83 cm^2), density of 350 kg/m^3, surface area of 598 m^2/g (BET), pore diameter of 29.77 Å, and pore volume of 0.5 cc/g (BJH). The monolith structure was crushed (cACM) and sieved to a particle size of $1 < d_p < 3$ mm prior to the catalytic reactions.

2.3. Catalyst Preparation. The base granular activated carbon (Base-GAC) was washed until neutral pH (3×) to eliminate any contaminants (initial pH was ∼5.8). Sulfuric acid

https://doi.org/10.1021/acs.iecr.2c00086
Ind. Eng. Chem. Res. 2022, 61, 3928−3940

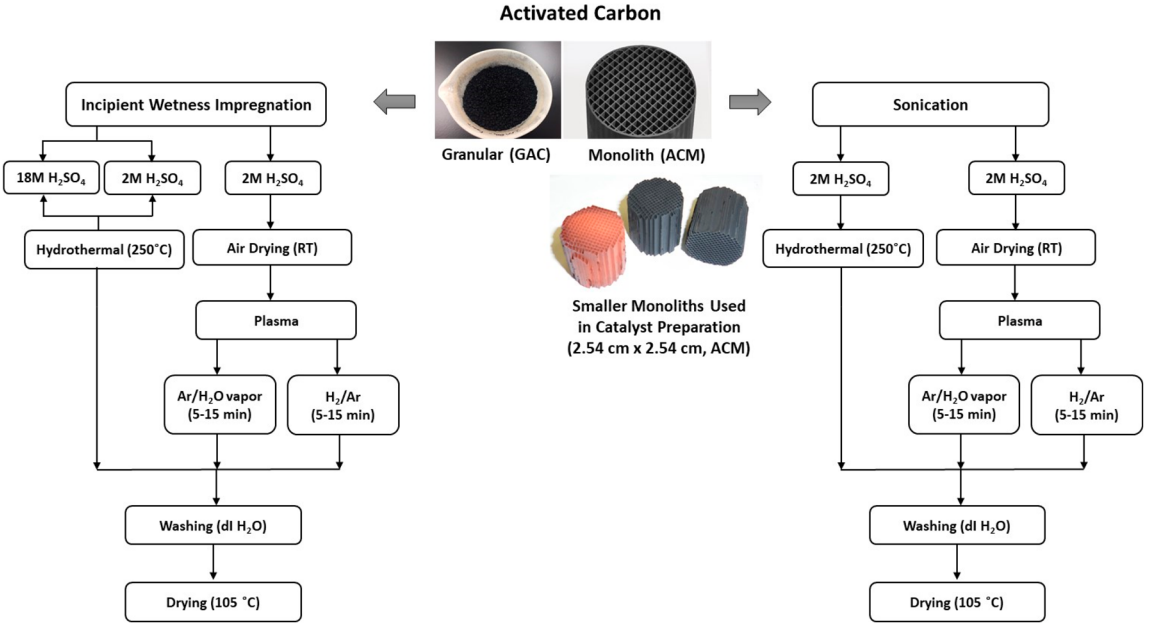

Figure 1. Schematic depicting the catalyst preparation methods of the hydrothermal and plasma sulfonated granular activated carbon (GAC) and activated carbon monolith (ACM: 2.54 × 2.54 cm cores) catalysts (RT: room temperature, dI H_2O: deionized water). Iron oxide impregnated ACM (red to orange ACM) was not used but is shown to demonstrate ability to deposit active metal oxides. The larger monolith (5.1 cm diameter) was not used in the work and is shown as example of monolith scale-up.

(18 or 2 M) was introduced into the GAC by incipient wetness impregnation at 1.75 mL/g catalyst (1.75:1 [v/w] sulfonating agent:carbon ratio), a little excess than the pore volume of 1.23 mL/g, to ensure all particles were sufficiently wetted. The monolith cores (Base-ACM) were immersed into 2 M H_2SO_4 (100 mL) and sonicated at 30 °C for 30 min. After sonication, the cores were removed. Excess liquid was removed by blotting, and the solution was weighed to determine the volume of impregnated sulfonating solution. A sulfonating agent to carbon ratio of 0.62:1 [v/w] was calculated for the ACM process. A schematic depicting the catalyst preparation methods is presented in Figure 1.

2.3.1. Hydrothermal Synthesis (HT). The GAC and ACM catalysts subjected to incipient wetness or wetness impregnation with sonication respectively, were treated hydrothermally at 250 °C in a muffle furnace (Fisher Scientific) for 12−16 h. These catalysts are named GAC-HT-18M, GAC-HT-2M, and cACM-HT-2M. Hydrothermal treatment of the monolith using 18 M H_2SO_4 was avoided.

2.3.2. Plasma Treatment (PT). For plasma sulfonation, the GAC and ACM catalysts treated with dilute H_2SO_4 by incipient wetness or sonication respectively, were air-dried overnight. Plasma treatment was performed in a Harrick expanded plasma cleaner (PDC-001, 115 V, chamber size 150 × 170 mm, maximum radiofrequency power 30 W), connected to a vacuum pump (Edwards XDS 5). Plasma treatment was investigated with a mixture of argon and water vapor and 3% hydrogen balance argon (inflammable) at three different time points of 5, 10, and 15 min (details in Supporting Information and Figure S1). These catalysts are named GAC-PT-Ar/H_2O-5,10, 15 min; GAC-PT-H_2/Ar-5,10,15 min; cACM-PT-Ar/H_2O-5,10,15 min; and cACM-PT-H_2/Ar-5,10,15 min. A comparison of the two plasma treatments is provided in theSupporting Information.

2.3.3. Washing. Post-treatments, all sulfonated catalysts were washed (the ACM cores were crushed prior to washing) with deionized water (25−50 mL/g catalyst) at room temperature to remove traces of excess acid (H_2SO_4), and to ensure the catalytic activity was solely due to the sulfonated carbon. Washing (8−12×, 1 h washes) was carried out until the filtrate displayed a constant pH, (approximately 5.2−5.5 for the GAC and 4.0 for the ACM catalysts). Care was exercised to minimize particle attrition. Postwashing, all catalysts were dried in a hot air oven at 105 °C overnight and stored for further experiments.

2.4. Catalyst Characterization. The surface area of the hydrothermal and plasma sulfonated carbons was measured by N_2 adsorption (Nova LX4, Anton Parr, U.S.A) and a 3-point BET analysis. Scanning transmission electron microscopy (STEM) imaging was performed on a Hitachi SU-9000. Subsequent Energy-dispersive X-ray spectroscopy (EDS) analysis was conducted on a ThermoFisher Teneo with an Oxford Xmax EDS detector. The sulfur (S) and phosphorus (P) content on the catalysts was quantified by microwave digestions followed by inductively coupled plasma-optical emission spectroscopy (ICP-OES) analysis. The samples were digested following EPA Method 3052, and the final solutions were analyzed for S and P following EPA Method 200.8 by ICP-OES (Spectro Arcos FHS16, Germany). Sulfonic acid density was estimated from the sulfur content, assuming all S atoms were in the $-SO_3H$ form. Fourier transform infrared (FTIR) analysis (1 mg of catalyst with 300 mg of KBr) was performed to qualitatively assess the formation of sulfonic acid groups on the carbon catalysts using a Thermo Scientific Nicolet 6700 (4000−399 cm^{-1}). X-ray photoelectron spectroscopy (XPS) analysis was performed on a Thermo Scientific K-Alpha XPS system with a monochromatic Al K_α (1486.6 eV) X-ray source (details for all methods are in Supporting Information).

2.5. Analytical Methods. Standard solutions of 2HIBA and ethyl-2-hydroxyisobutyrate (E-2HIBA) were prepared in ethanol. Each standard was analyzed in triplicate to determine

https://doi.org/10.1021/acs.iecr.2c00086
Ind. Eng. Chem. Res. 2022, 61, 3928−3940

Scheme 1. Main Reaction and Possible Byproducts, Diethyl Ether and Ethylene

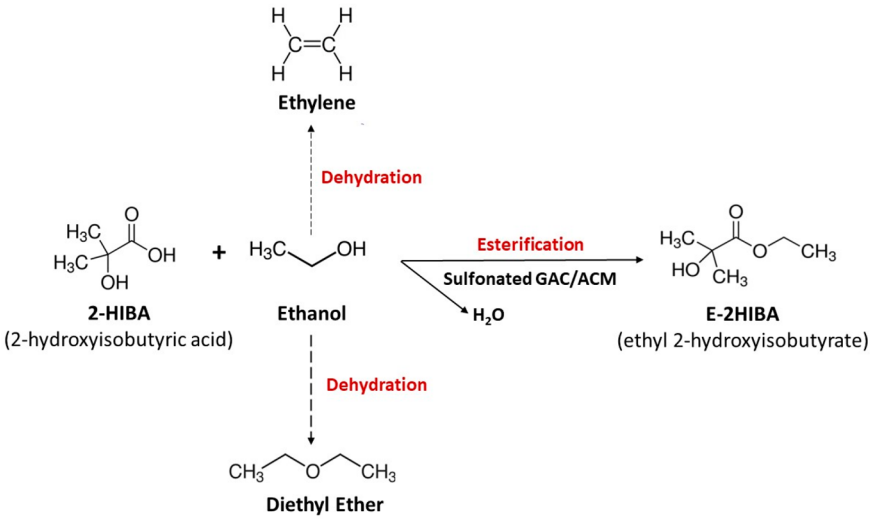

Table 1. Physical and Reaction Characteristics of the Sulfonated Carbons and Amberlyst-15[a]

catalyst	surface area (m^2/g)	phosphorus (%)	SO_3H density[k] (mmol/g)	reaction rate (0.25 h) (mmol/g/min)	TOF (0.25 h) (min^{-1})[c,d]	TOF (0.75 h) (min^{-1})[c,d]
Base-GAC[b]	1490	1.5				
GAC-HT-18M[e]	453	0.5	0.164 ± 0.007	0.325 ± 0.036	1.985 ± 0.23	0.93 ± 0.01
GAC-HT-2M[f]	1015	1.3	0.089 ± 0.028	0.0895 ± 0.071	1.0 ± 0.79	1.28 ± 0.11
GAC-PT-Ar/H_2O-15 min[g]	1385	0.9	0.006 ± 0.001	0.0715 ± 0.012	11.9 ± 2.9	9.24 ± 2.08
Base-cACM[b]	598	0.04				
cACM-HT-2M[h,i]	550	0.04	0.124 ± 0.003	0.09 ± 0.004[i]		0.725 ± 0.03[i]
cACM-PT-Ar/H_2O-10 min[j,i]	462	0.04	0.015 ± 0.000	0.03 ± 0.013[i]		2.02 ± 0.84[i]
Amberlyst-15	38	0.00	2.365 ± 0.446	0.325 ± 0.00013	0.138 ± 0.000	0.0615 ± 0.001

[a]Reaction conditions: temperature 150 °C, residence time includes heat-up time, catalyst loading 1 g, reaction volume 20 mL, and 2-HIBA concentration 40g/L. [b]Base-GAC and Base-cACM are the untreated GAC and cACM (crushed monolith). [c]Except where noted, the value in the parentheses for reaction rate and TOF are the contact times. [d]TOF, turnover frequency based on the 2-HIBA reaction rate and SO_3H density. [e]GAC treated with 18 M H_2SO_4 by incipient wetness impregnation, followed by hydrothermal treatment at 250 °C. [f]GAC treated with 2 M H_2SO_4 by incipient wetness impregnation, followed by hydrothermal treatment at 250 °C. [g]GAC treated with 2 M H_2SO_4 by incipient wetness impregnation, followed by plasma treatment with argon−H_2O vapor for 15 min. [h]Crushed ACM treated with 2 M H_2SO_4 by sonication, followed by hydrothermal treatment at 250 °C. [i]1.25 h including heat-up time. [j]Crushed ACM treated with 2 M H_2SO_4 by sonication, followed by plasma treatment with argon-H_2O vapor for 10 min. [k]Based on elemental analysis.

the standard deviations (SD). Liquid sample collected from the reactor was analyzed using HP 5890 Series II gas chromatography equipped with a flame ionization detector (GC-FID) and a HP Innowax column (30 m × 0.25 mm × 0.25 mm). The GC-FID was operated with the method of inlet temperature 240 °C, detector temperature 250 °C, initial oven temperature of 45 °C for 2.5 min followed by a ramp of 10 °C/min for 21 min, and then held at 230 °C for 4 min. One microliter of each sample was injected on the GC-FID in triplicate.

2.6. Catalytic Reactions. Catalytic esterification of 2-hydroxyisobutyric acid was performed in 75 mL autoclave batch reactors (Parr Series 5000 Multiple Reactor System). A working volume of 20 mL (40 ± 2 g L^{-1} 2HIBA in ethanol) and catalyst was mixed using a magnetic stir bar (725 rpm). Details on reaction conditions can be found in the Supporting Information. All experiments were performed in duplicate. Scheme 1 shows the main reaction and possible byproducts, diethyl ether and ethylene. Esterification reaction rates (mmolg-cat^{-1} h^{-1}), 2-HIBA conversion (mol converted/mol initial 2HIBA), E-2HIBA yield (mol produced/mol initial 2HIBA) and selectivity (mol produced/mol 2HIBA remaining and E-2HIBA) were calculated using the batch data as previously reported.[7] The turnover frequency (TOF, min^{-1}) was estimated from the reaction rate ($mmolg^{-1}min^{-1}$) and acid site density ($mmolg^{-1}$). In calculating the reaction rates and TOF, the heat-up time (15 min) was included in the contact time (Table 1).

2.7. Statistical Analysis. All 2-HIBA esterification reactions were performed in duplicate, while ICP-OES and GC-FID analyses were performed in triplicate and reported as the mean and sample standard deviation. Sample standard deviation was calculated from the range (R) for small sample size (n) for reaction rate, TOF, yield, and conversion (for $n \leq 5$, R/d_2, where $d_2 = 1.128$).[26] In the analysis between two means for the TOF, E-2HIBA yield and 2-HIBA conversion, a student t test was performed, assuming the null hypothesis, and the level of significance (α) is reported.

3. RESULTS AND DISCUSSION

In the following sections, catalyst characterization is correlated with structural and physical properties, and catalytic activity. 2-

https://doi.org/10.1021/acs.iecr.2c00086
Ind. Eng. Chem. Res. 2022, 61, 3928−3940

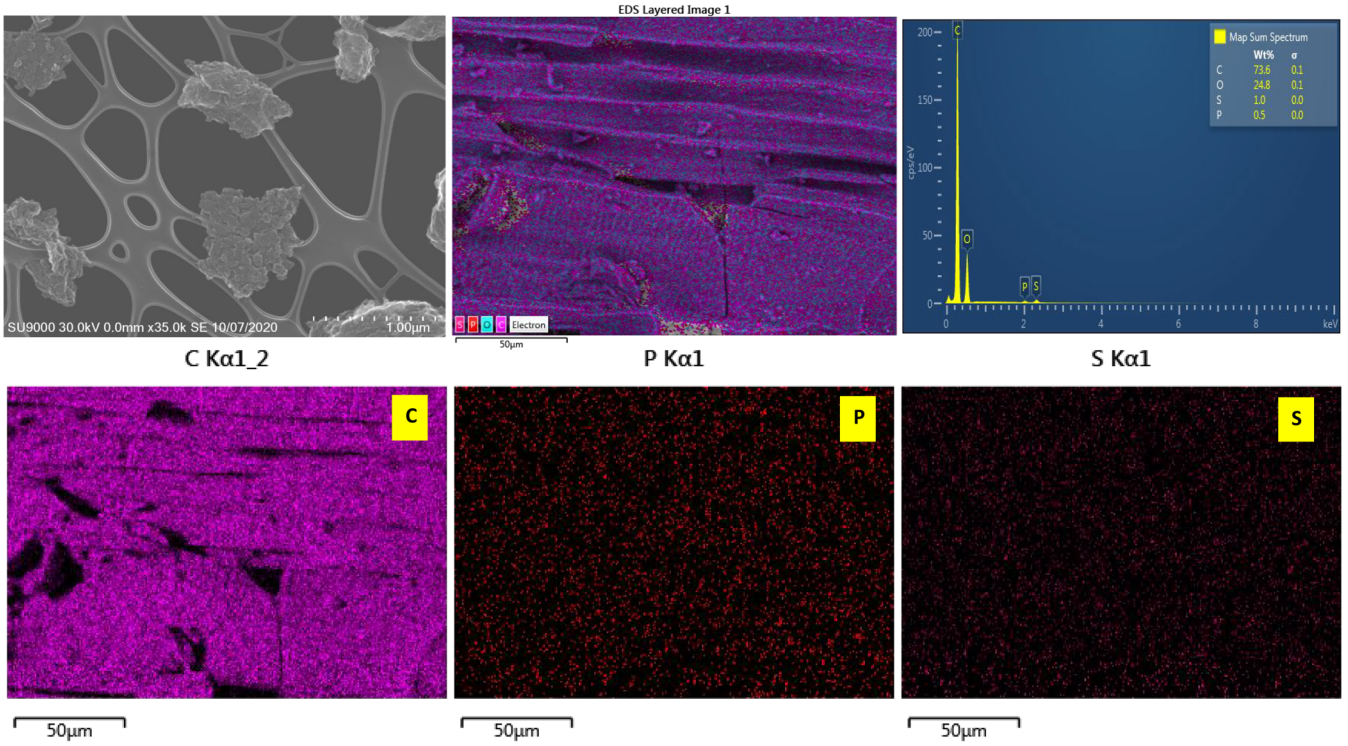

Figure 2. STEM-EDS images of GAC-HT-18M catalyst.

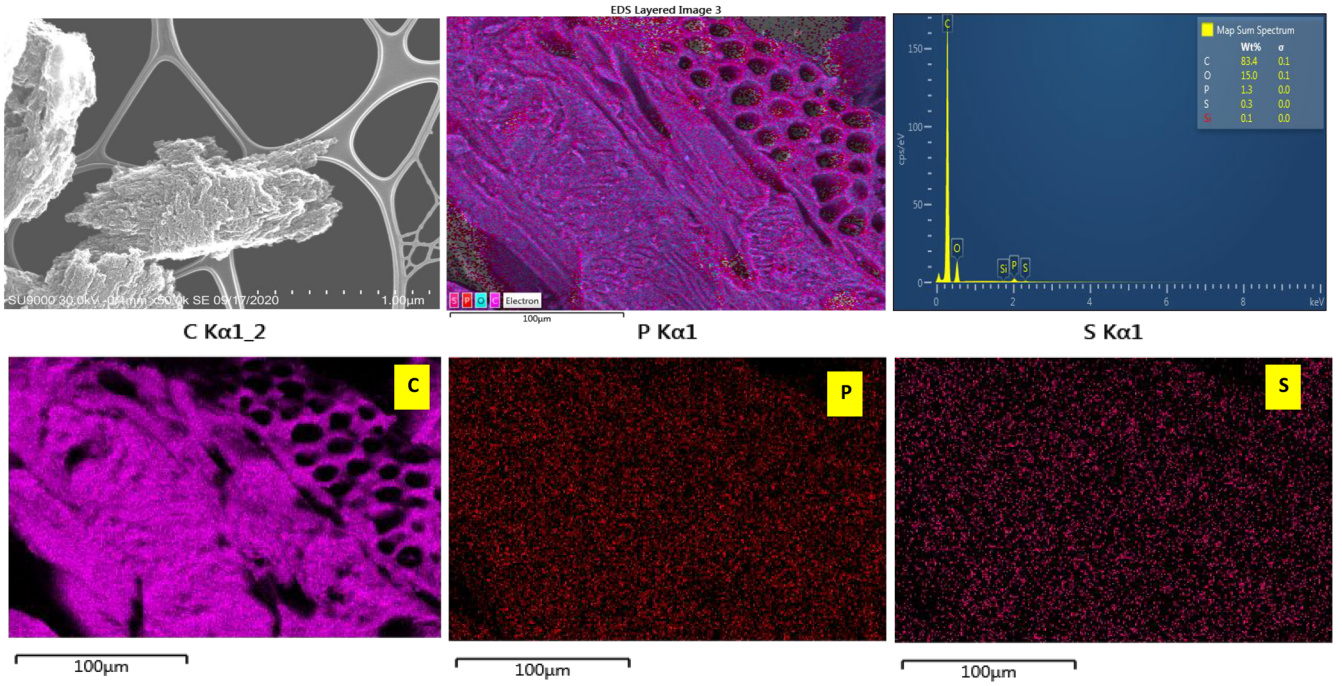

Figure 3. STEM-EDS images of GAC-HT-2M catalyst.

HIBA batch esterification results are compared between the untreated base materials, and the hydrothermal and plasma sulfonated carbons. Catalyst reusability as well as reaction studies are also analyzed.

3.1. Catalyst Structure. Untreated GAC and cACM had surface areas of 1490 and 598 m^2/g, respectively, with limited reduction in surface area for plasma treatment and dilute H_2SO_4 impregnation (Table 1). Like previous work, a surface area reduction of 31.9% in GAC-HT-2M and 69.6% in the GAC-HT-18M was observed, due to sulfonation and oxidation reactions on the carbon catalysts.[15,27−29] Plasma sulfonation of GAC caused a small decrease (7.0%) in surface area, providing a larger surface area for catalytic reactions, indicating plasma treatment did not significantly affect bulk structure. A lower reduction in surface area for ACM versus GAC was observed (8% for HT). Plasma treatment of ACM did generate larger

https://doi.org/10.1021/acs.iecr.2c00086
Ind. Eng. Chem. Res. 2022, 61, 3928−3940

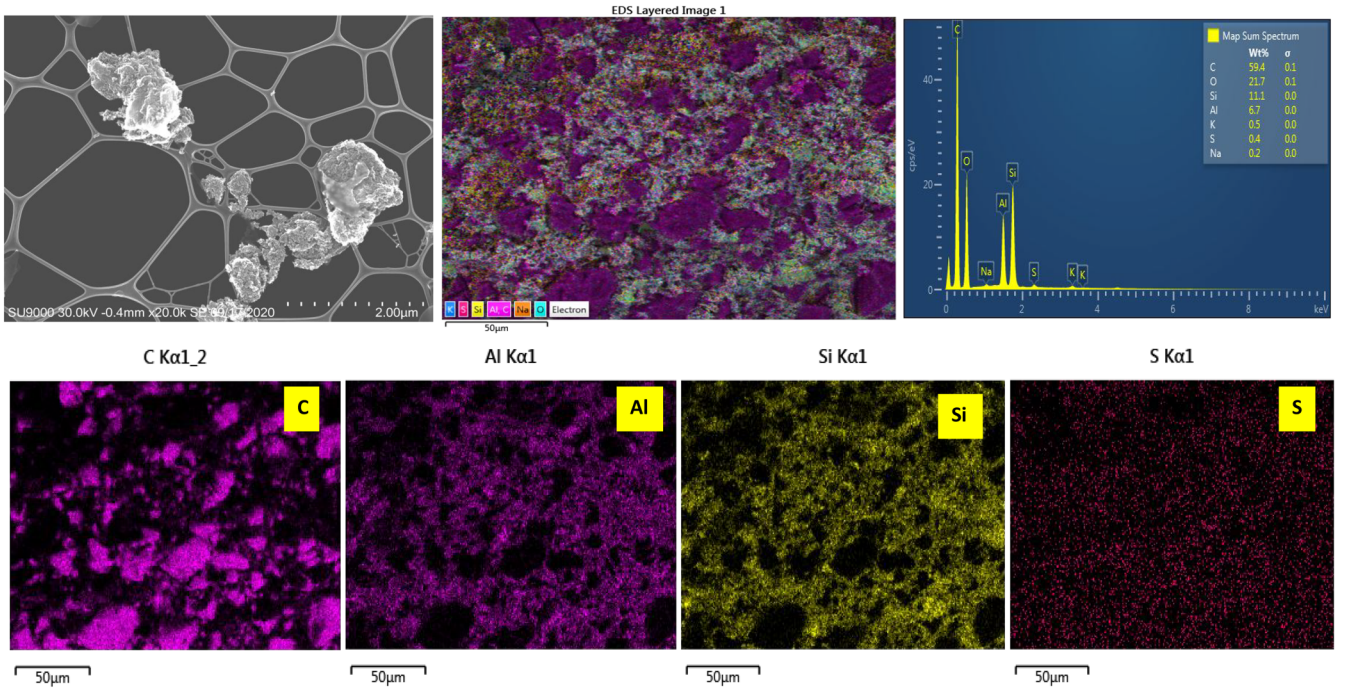

Figure 4. STEM-EDS images of cACM-HT-2M catalyst.

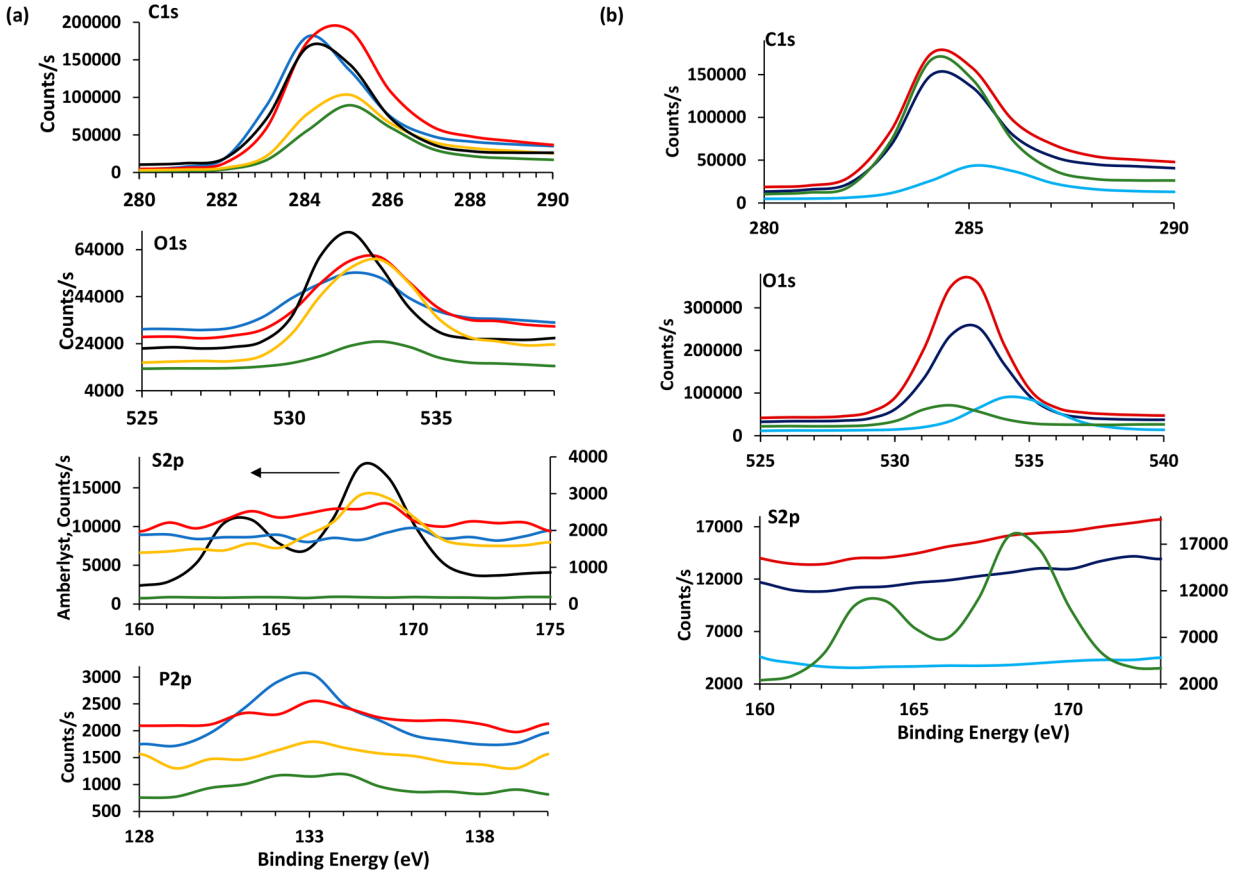

Figure 5. XPS analysis of (a) Base-GAC (blue), GAC-HT-2M (red), GAC-HT-18M (yellow), GAC-PT-Ar/H2O-15 min (green) and Amberlyst-15 (black) and (b) Base-cACM (dark blue), cACM-HT-2M (light blue), cACM-PT-Ar/H2O-10 min (red) and Amberlyst-15 (green).

surface area reduction than GAC (~23%), potentially due to its open structure and better plasma exposure. Amberlyst-15 has a much lower surface area (38 m^2/g) and limited porosity.[30]

https://doi.org/10.1021/acs.iecr.2c00086
Ind. Eng. Chem. Res. 2022, 61, 3928−3940

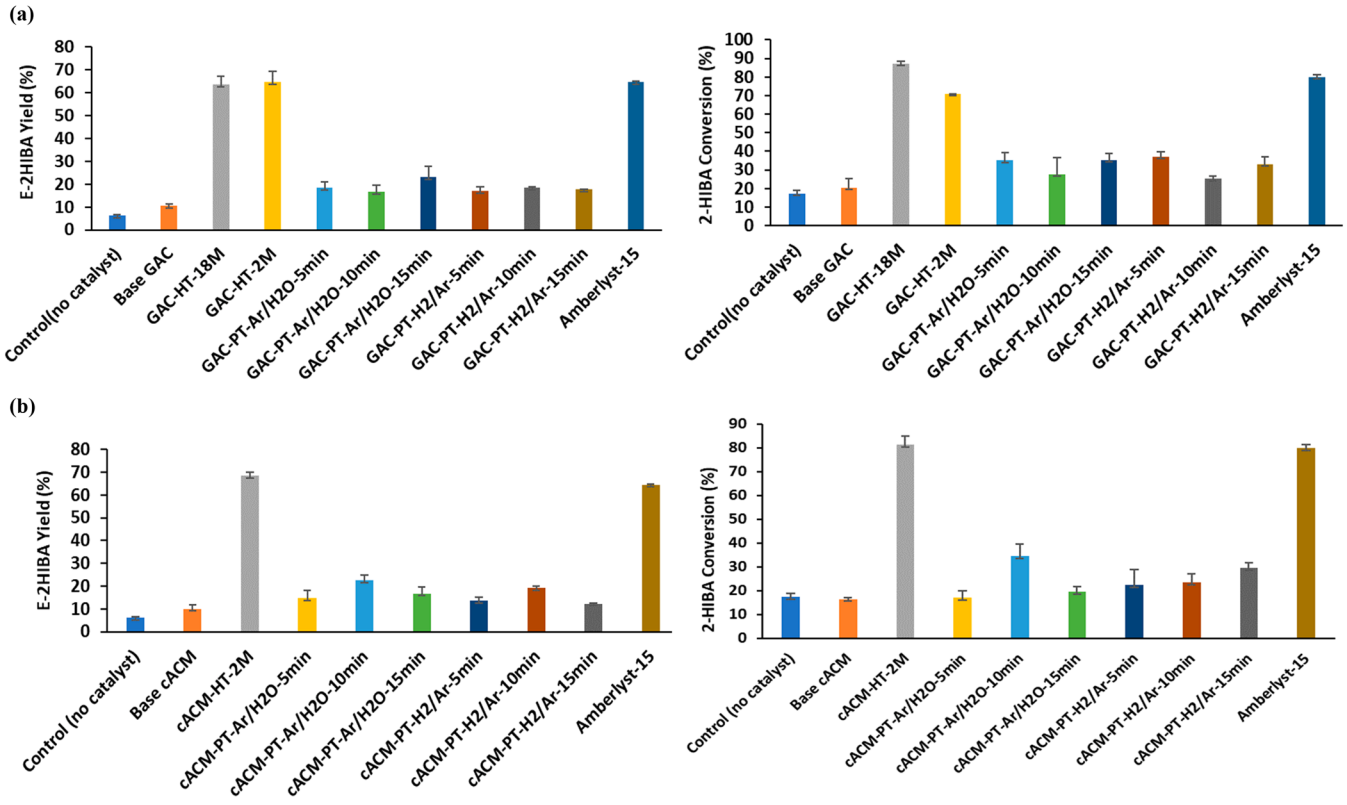

Figure 6. E-2HIBA yield and 2-HIBA conversion for the hydrothermal and plasma sulfonated (a) GAC and (b) cACM catalysts vs Amberlyst-15 in the batch esterification of 2-HIBA with ethanol. Reaction conditions: temperature 150 °C, residence time 1 h, catalyst loading 1 g, reaction volume 20 mL and 2-HIBA concentration 40g/L.

Elemental mapping by STEM-EDS revealed base-GAC had a phosphorus (P) content of 1.5%, indicating chemical activation by phosphoric acid (Figure S2, Table 1).[31] Phosphate sites were also displayed on the hydrothermally sulfonated GAC catalysts (GAC-HT-18M and GAC-HT-2M) (Figures 2 and 3). EDS analysis indicated a sulfur (S) content of 0.3% and 1% on the GAC-HT-2M and the GAC-HT-18M, respectively, uniformly distributed on the catalyst surface. The P content decreased to 1.3% and 0.5% in GAC-HT-2M and GAC-HT-18M, respectively. STEM images of base-cACM (Figure S3) indicate a porous network, with silica and aluminum surrounding the carbon, attributed to the ceramic binder used to manufacture the ACM. A sulfur content of 0.4% was detected on the cACM-HT-2M (Figure 4), evenly distributed on the catalyst surface. EDS analysis of GAC-PT-Ar/H_2O-15 min and cACM-PT-Ar/H_2O-10 min could not detect any sulfur, indicating its concentration was below the detection limit of the EDS (<0.1%).

ICP-OES analysis was performed to quantify sulfur, and sulfonic acid densities were estimated assuming all S corresponded to $-SO_3H$ groups (Table 1). The Base-GAC and cACM did not contain any S/$-SO_3H$ acid groups prior to sulfonation. Sulfonic acid densities of 0.16 and 0.09 mmol/g were obtained for GAC-HT-18M and GAC-HT-2M, respectively, which indicate the incipient wetness impregnation method results in lower acid densities compared to traditional methods. An H_3PO_4-activated carbon sulfonated with concentrated H_2SO_4 (15 mL/g catalyst) under reflux generated a sulfonic acid density of 0.24 mmol/g (92 °C, 7 h).[32] Carbon refluxed in 6 M H_2SO_4 generated an $-SO_3H$ density lower than 0.1 mmol/g, which was similar to our results.[33] Hydrothermal sulfonation of ACM (cACM-HT-2M) resulted in a sulfonic acid density of 0.12 mmol/g, again similar to the literature.[29] The sulfur content of the plasma sulfonated GAC (GAC-PT-Ar/H_2O-15 min) and cACM (cACM-PT-Ar/H_2O-10 min) were found to be 0.02% and 0.05% respectively, corresponding to sulfonic acid densities below 0.1 mmol/g.

FTIR spectra indicated a peak at 1047−1049 cm^{-1} and a broad band between 1254 and 1174 cm^{-1} in all the GAC catalysts (Figures S5 and S6, Table S1). The band between 1000 and 1300 cm^{-1} is characteristic of phosphorylated carbons and attributed to stretching vibrations of hydrogen bonded P═O, O—C stretching in P—O—C linkage, and to P═OOH.[31,34] The hydrothermal (cACM-HT-2M) and plasma treated ACM (cACM-PT-Ar/H_2O-10 min) show a distinct peak at 1059 cm^{-1} attributed to S═O stretching vibrations of $-SO_3H$ groups; O═S stretching at 1042 cm^{-1} is reported in a sulfonated graphene oxide monolith.[35] Peaks at 1030 and 1210 cm^{-1} are attributed to symmetric and asymmetric stretching vibrations of the SO_3^{-1} group, respectively.[36] The peak at 1188 cm^{-1} has also been assigned to S═O symmetric stretching vibration and the peaks at 1036 cm^{-1} assigned to S═O and SO_3^{2-} stretching vibrations, respectively.[37,38]

Because $-SO_3H$ signatures, especially in the sulfonated GAC catalysts, were not clear, XPS analysis was performed (Figure 5, Table S2). Prominent peaks for oxygen and carbon, and weak peaks for sulfur were observed at binding energies of 284.5, 532, and 168 eV, respectively, in all treated catalysts.[38] The C 1s peak at 284.5 eV corresponds to polycyclic aromatics (C═C), and the peaks at 285.2 and 286.0 eV can be assigned to aliphatic hydrocarbons (C—C) and C—O—C, respec-

https://doi.org/10.1021/acs.iecr.2c00086
Ind. Eng. Chem. Res. 2022, 61, 3928−3940

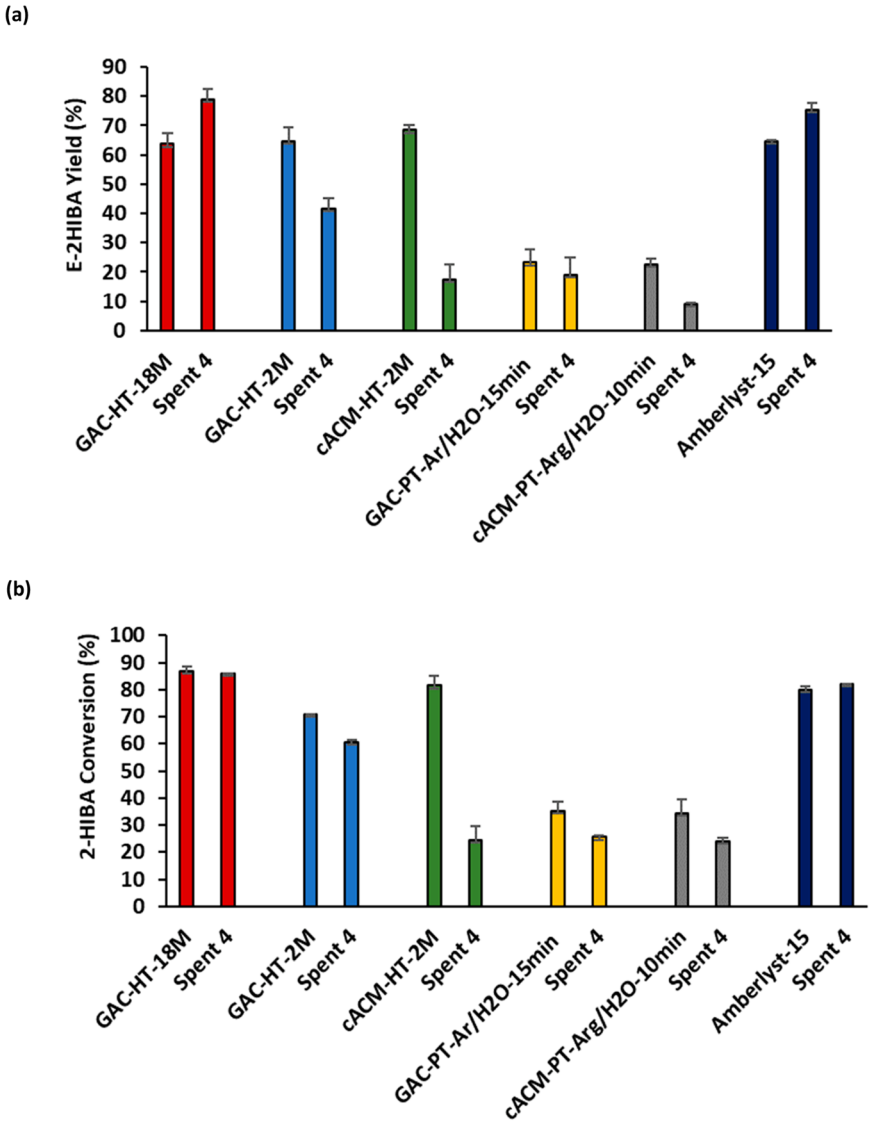

Figure 7. (a) E-2HIBA yield and (b) 2-HIBA conversion in catalyst reuse studies with the hydrothermal and plasma sulfonated GAC and cACM catalysts compared to Amberlyst-15.

tively. Peaks for carbonyl C═O and carboxyl O—C═O groups appear at 287.2 and 288.7 eV, respectively. The peak at 532.9 eV is assigned to O—H, C═O at 531.7 eV and bridging C—O—C at 533.7 eV.[37] The sulfur peaks at 164.0 and 165.2 eV correspond to S $2p_{3/2}$ and S $2p_{1/2}$ of thiophenic sulfur respectively (−C—S—C−), and the peak at 168.0 eV can be assigned to the SO_3H group. These sulfur peaks have also been observed in XPS analyses of sulfonated carbon materials.[38] The two peaks for sulfur were prominent in the hydrothermal and plasma sulfonated GAC catalysts (relative to Base-GAC) and Amberlyst-15 but were not as evident in the ACM catalysts (Figure 5). Additionally, the Base-GAC had one broad P 2p peak at 133 eV. Two peaks at 132.7 and 134.8 eV were apparent in the hydrothermal and plasma sulfonated GAC catalysts and can be assigned to P—O—C and P—O (phosphate).[39]

Argon−water vapor plasma has been shown to alter C 1s binding energy in carbon materials. It is reported that a small decrease in the C 1s peak at 285.0 eV, and increase in the peaks at 286.5, 287.7, and 289.1 eV, indicate a decrease in concentration of C—C/C—H bonds and increase in oxygen containing groups (C—O, C═O, O—C—O and O—C═O) with increasing water vapor concentration.[40] It is theorized that argon−water vapor plasma promotes surface hydrogen abstraction by OH radicals and O atoms.[40] We observed similar results with our Ar/H_2O vapor treated GAC and ACM catalysts. With GAC-PT-Ar/H_2O-15 min, we noted a clear shift in the C 1s peak at 284 eV (C═C) to 285 eV (oxygenated carbon). This shift was prominently noted in the GAC-HT-2M and GAC-HT-18M catalysts (Figure 5). The cACM-PT-Ar/H_2O-10 min catalyst had a shoulder at 285 eV indicative of partial surface oxidation and incorporation of oxygen groups, compared to the cACM-HT-2M, which had a prominent peak at 285 eV.

3.2. Catalytic Esterification. Esterification studies were performed to compare the catalytic performance of the plasma and hydrothermally sulfonated carbons (GAC and ACM) with Amberlyst-15 (150 °C, 1 h, 1 g of catalyst). Reaction conditions were chosen based on preliminary experiments at conditions ranging from 100 to 150 °C, 0.5−3 h, and catalyst loadings of 0.25 and 1 g, and with both 1 and 2 M H_2SO_4 treated GAC (plasma and hydrothermal). Preliminary

https://doi.org/10.1021/acs.iecr.2c00086
Ind. Eng. Chem. Res. 2022, 61, 3928−3940

esterification reactions indicated higher conversions with 2 M H_2SO_4 treated carbons, and these catalysts were selected for further studies (data not shown) at 40 g/L of 2-HIBA in excess ethanol (~44:1 ethanol to 2HIBA molar ratio).

In the absence of catalyst, E-2HIBA yield and 2-HIBA conversion were 6.2% and 17.4%, respectively, indicating that at 150 °C heat alone can drive the reaction (Figure 6). With both base GAC and cACM, the E-2HIBA yields were about 10%, while the 2-HIBA conversions were 20.5% and 16.5%, respectively. Weak acid sites (−COOH) and $-PO_4$ sites in GAC may have contributed to esterification activity and a larger catalyst surface area may have generated higher conversion with the Base-GAC. The hydrothermally sulfonated ACM (cACM-HT-2M) displayed the maximum ester yield of 68.5% among all catalysts, and a 2-HIBA conversion of 81.5% in comparison to an E-2HIBA yield of 64.7% (α = 0.05−0.1) and 2-HIBA conversion of 80% with Amberlyst-15. These results suggest wet impregnation with dilute H_2SO_4 coupled with sonication and thermal activation can generate solid acid carbon monolith catalysts. Our results compare with a report using graphene oxide (the hazardous and potentially explosive Hummer's method is typically used to synthesize graphene).[41] Esterification of levulinic acid with benzyl alcohol using a sulfonated graphene oxide monolith generated a conversion of 97% at 110 °C and 90 min.[35]

The two hydrothermally treated GAC catalysts, GAC-HT-18M and GAC-HT-2M, gave similar ester yields of 63.7% and 64.7% with 2-HIBA conversions of 87% and 71%, respectively. These results indicate that the catalytic performance of the GAC-HT-2M and cACM-HT-2M was similar to Amberlyst-15 (150 °C, 1 h) and reports in the literature. Esterification of glycerol with acetic acid using a sulfonated carbon generated a maximum glycerol conversion of 80% at 150 °C after 5 h.[33]

Among the 3% H_2/Ar plasma treated GAC catalysts, a maximum E-2HIBA yield of 18.5% was observed at the 10 min treatment time (2-HIBA conversion was 25.1%), although varying the plasma treatment duration did not significantly impact the ester yield. With the Ar/H_2O vapor treated GAC catalysts, the E-2HIBA yield increased from 18.6% to 23.2% on increasing the exposure time to 15 min (2HIBA conversion and E-2HIBA selectivity were 35.3% and 26.8%, respectively). Of the 3% H_2/Ar treated ACM catalysts, a maximum E-2HIBA yield of 19.3% and selectivity of 20.2% were obtained at the 10 min treatment time (2-HIBA conversion was 23.5%). Although prolonged plasma exposure (15 min) led to an increase in 2-HIBA conversion, a decrease in E-2HIBA yield and selectivity were observed, with byproduct formation. With the Ar/H_2O vapor plasma, at the 10 min treatment time, a maximum 2-HIBA conversion, E-2HIBA yield and selectivity of 34.5%, 22.6%, and 25.6%, respectively, were obtained.

For all sulfonated ACM catalysts, with both plasma treatments, an increase in E-2HIBA yield and selectivity, as well as 2-HIBA conversion were observed on increasing the plasma duration from 5 to 10 min. Similar results were obtained with the sulfonated GAC catalysts, although the difference was more evident on increasing the exposure time to 15 min. It has been found that nonhomogeneous plasma modification is likely for shorter treatment durations or low ion doses, as the ion dose may not be uniform on the catalyst surface.[42] Increasing the plasma exposure time to 10 and 15 min were found to be optimal for the ACM and GAC catalysts, respectively. Increasing the treatment time to 15 min for the sulfonated ACM catalysts, resulted in a decrease in ester yield, selectivity, and substrate conversion, which could be attributed to byproduct formation.

Similar E-2HIBA yields and 2-HIBA conversions were obtained with both the GAC and ACM using Ar/H_2O vapor as carrier gas, at different treatment times of 15 and 10 min, respectively. The monolith core was treated intact during the plasma exposure and crushed prior to the catalytic reactions, which could be the reason for the shorter exposure time requirement. Because the monolith is a uniform block (2.54 × 2.54 cm) with open channels, it may have experienced better catalyst-gas-plasma interaction in comparison to the GAC during the plasma treatment.[43] Because the GAC-PT-Ar/H_2O-15 min and cACM-PT-Ar/H_2O-10 min were the most catalytically active plasma sulfonated catalysts, reaction analysis and catalyst reuse studies were performed with these catalysts and the hydrothermal GAC and ACM catalysts (GAC-HT-18M, GAC-HT-2M, cACM-HT-2M).

3.3. Catalyst Reuse. Catalyst reuse studies were carried out for 4 cycles (5 h, Figure 7). Both GAC-HT-18M and Amberlyst-15 retained 100% of their catalytic activity, and an increase in E-2HIBA yield from the first to fourth spent run was noted. Analysis of the carbon balance resulted in over 100% carbon recovery, indicating carry over from the previous spent run. This could be because the catalysts were recovered and reused as is, without washing, causing any ester bound to the catalyst to leach out in the subsequent run. The GAC-HT-2M retained 85% of its catalytic activity with a 35.6% loss in ester yield (41.65 vs 64.65 g/L). However, cACM-HT-2M depicted a decrease in catalytic activity with 2-HIBA conversion decreasing from 81.5% to 24.5% in the fourth spent run (~70% decrease). To understand the loss in catalytic activity, we performed STEM-EDS on the spent (4th run) hydrothermal GAC and cACM catalysts. EDS analysis of the spent GAC-HT-2M indicated stability of SO_3H groups in the hydrothermal GAC catalysts as the sulfur content remained constant at 0.3%. However, a decrease in sulfur content from 0.4% to 0.2% was observed in the cACM-HT-2M, confirming loss of SO_3H groups and reduction in activity (Figure S4). Similar results were observed using a hydrothermally synthesized sulfonated carbonaceous monolith in the acetalization of benzaldehyde.[44] In this work a significant loss in catalytic activity with each reaction cycle was reported, and one carbon catalyst only retained 31% of its initial catalytic activity (conversion decreased from 87.1% with the fresh catalyst to 27.3% in the fourth spent run).[44] ICP-OES analysis on the spent catalysts confirmed that catalyst deactivation was due to sulfur leaching.[44] Plasma sulfonated GAC (GAC-PT-Ar/H_2O-15 min) retained 75% of its catalytic activity, and 81.8% of the E-2HIBA yield obtained with the fresh catalyst, similar to previous work with in-solution (1 M H_2SO_4) plasma sulfonated carbon black (98% catalytic activity after 3 spent cycles).[14] The surface area of this catalyst was much lower (40 m^2/g)[14] in comparison to our plasma sulfonated GAC, GAC-PT-Ar/H_2O-15 min (1385 m^2/g). Our results indicate that the plasma process imparted good stability and reusability to the GAC, and because the catalyst has a high surface area, its performance can be enhanced by modifying the plasma parameters, to obtain higher acid site densities. Similar to the hydrothermal cACM catalyst, the plasma sulfonated cACM also showed a decline in catalytic activity, with a 59.3% and 30.4% decrease in E-2HIBA yield and 2-HIBA conversion, respectively. Despite the lower ester yield and 2-HIBA conversion, the plasma sulfonated cACM performed better in

https://doi.org/10.1021/acs.iecr.2c00086
Ind. Eng. Chem. Res. 2022, 61, 3928−3940

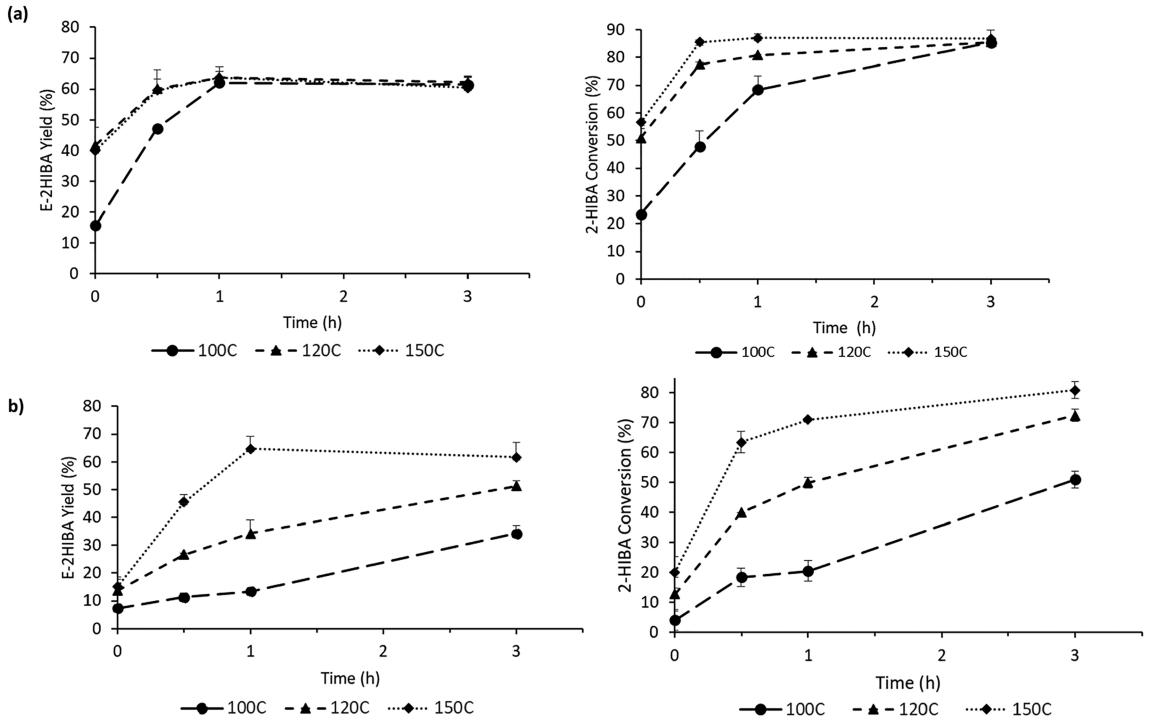

Figure 8. Reaction studies depicting the E-2HIBA yield and 2-HIBA conversion for the (a) GAC-HT-18M and (b) GAC-HT-2M at temperatures of 100−150 °C and residence times ranging from 0.5 to 3 h.

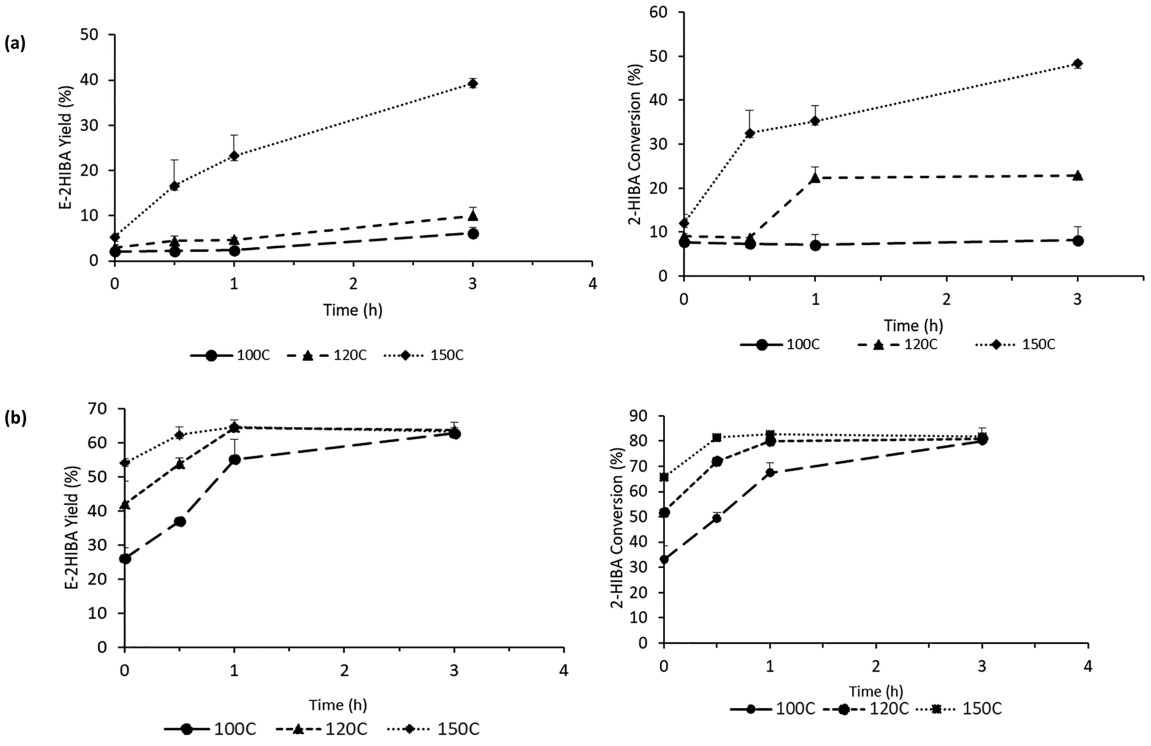

Figure 9. Reaction studies depicting the E-2HIBA yield and 2-HIBA conversion for (a) GAC-PT-Ar/H_2O-15 min and (b) Amberlyst-15 at temperatures of 100−150 °C and residence times ranging from 0.5 to 3 h.

comparison to the hydrothermally sulfonated ACM in terms of catalyst stability, indicating stability conferred by the plasma. The sulfonated GAC catalysts also displayed greater catalyst stability in comparison to the monolithic catalysts, which may be attributed to phosphoric acid chemical activation of the carbon. Phosphorylated activated carbon fiber catalysts are reportedly thermally stable for 12 h at 350 °C in air.[45] Catalytic esterification of oleic acid with methanol has recently been reported using phosphorylated carbon.[1] The thermally stable $-PO_4$ groups noted in the GAC catalysts may have promoted

https://doi.org/10.1021/acs.iecr.2c00086
Ind. Eng. Chem. Res. 2022, 61, 3928−3940

adsorption of 2-HIBA and synergistically enhanced esterification at the $-SO_3$ sites.

3.4. Reaction Studies. From the catalyst reuse studies, four sulfonated carbon catalysts including the GAC-HT-18M, GAC-HT-2M, GAC-PT-Ar/H_2O-15 min, and Amberlyst-15 were found to be the most stable, retaining over 80% catalytic activity. Additional reaction studies were performed with these catalysts to determine the effect of temperature (100,120,150 °C) and residence time (0.5,1,3h) on E-2HIBA yield and 2-HIBA conversion (Figures 8 and 9). Some product was formed at time zero, with the GAC-HT-18M and Amberlyst-15 displaying an increase in 2-HIBA conversion from 23.5% to 56.6%, and 33.1% to 65.7% on increasing the temperature from 100 to 150 °C. The 2-HIBA conversions for the GAC-HT-2M and GAC-PT-Ar/H_2O-15 min at time zero were less than 10% (reported conversions are after the time required to reach operating temperature, 15 min).

With all the four catalysts, increasing both the temperature and residence time increased 2-HIBA conversion and E-2HIBA yield, indicating 2-HIBA reaction rates were lower at 100 °C and increased with temperature up to 150 °C. With both GAC-HT-18M (Figure 8) and Amberlyst-15 (Figure 9), maximum E-2HIBA yields of 64−65% were obtained at 120 °C and 1 h residence time. Increasing the temperature to 150 °C led to an increase in the 2HIBA conversion and E-2HIBA selectivity (87% and 83% with GAC-HT-18M and 82.58 and 78.75% with Amberlyst-15). However, increasing the residence time to 3 h at 150 °C did not affect the ester yield or 2-HIBA conversion. Similar results have been reported for the esterification of oleic acid and methanol using a sulfonated carbon catalyst (oleic acid conversion of 97.9% at 1.5 h, and >2.5 h did not significantly affect conversion).[46]

With GAC-HT-2M, a maximum E-2HIBA yield of 64.65% was obtained at 150 °C and 1 h reaction time (2-HIBA conversion and E-2HIBA selectivity were 71% and 68.75%, Figure 8). The 2-HIBA conversion and E-2HIBA selectivity increased to 81% and 76.4%, respectively, after 3 h (E-2HIBA yield was 61.7%). These results indicate that the GAC-HT-18M and Amberlyst-15 attained equilibrium around 120 °C, while the GAC-HT-2M attained equilibrium at 150 °C, at approximately 1 h of reaction time. Similar results were observed with a carbon catalyst synthesized using concentrated sulfuric acid under reflux (150 °C, glycerol conversion of 76% after 5 h).[36]

For all reactions, the carbon recovery was above 90%. About 5−10% of the recovered carbon in terms of percent peak area were two unknowns (retention times of 1.76 and 7.1 min). As reaction temperature increased and time progressed, the peak at 1.76 min increased, particularly with the hydrothermal GAC catalysts and Amberlyst-15. Sulfonated and phosphorylated carbons can catalytically dehydrate ethanol forming diethyl ether and ethylene, suggesting these compounds as possible byproducts.[47] The increase in 2-HIBA conversion with the GAC-HT-18M and Amberlyst-15 on increasing the temperature from 120 to 150 °C (1 h of residence time), and with the GAC-HT-2M on increasing the residence time to 3 h at 150 °C did not affect the ester yield, yet led to an increase in the formation of byproducts. We therefore concluded that reaction temperatures of 120 °C for the GAC-HT-18M and Amberlyst-15, and 150 °C for the GAC-HT-2M at 1 h of residence time were optimal for 2-HIBA esterification. With the GAC-PT-Ar/H_2O-15 min, the ester yield and hydroxyacid conversion increased with both temperature and residence time, and a maximum E-2HIBA yield of 39.29% and 2HIBA conversion of 48.29% were observed at reaction conditions of 150 °C and 3 h (E-2HIBA selectivity 43.17%). The slower esterification rate with the plasma sulfonated GAC catalyst can be attributed to the low sulfonic acid site density. Low sulfonic acid site density on the catalyst may indicate lower availability of H^+ ions in the solution, resulting in a decrease in both 2-HIBA conversion and esterification rate.[48]

Although the plasma treated carbons had lower reactions rates on a per mass basis (mmol/g-cat/min), TOF based on strong acid sites ($-SO_3H$) was significantly higher (Figure S7 and Table 1). For example, the TOF for GAC-PT-Ar/H_2O-15 min was 86−150× higher than Amberylyst-15 (α = 0.02−0.05) and 6−10× higher than GAC-HT-18M (α = 0.02−0.05). Notably, the TOFs for the GAC-HT-2M/18M and cACM-HT-2M are significantly larger than that of Amberlyst-15 (Table 1, α = 0.001 and Figure S7). There are two possible reasons; many of the Amberlyst acid sites may not be accessible and its nonpolar surface may inhibit 2HIBA adsorption. The low surface area of Amberlyst limits access to acid sites and the polar nature (−COOH, −C═O, −OH, $-PO_4$ sites) on the treated GAC and ACM probably promoted 2HIBA adsorption, relative to Amberlyst-15. Similar results have been observed in the esterification of oleic acid.[49] Mesoporous carbons grafted with benzenesulfonic acid had TOF's 5−7× greater than that of Amberlyst-15, yet lower strong acid density. These carbons also had greater total acid site densities than strong acid density, suggesting additional weak acid sites on the carbon (e.g., −COOH). The increased TOF was due to better dispersion of carbons in methanol via the weak acid sites and limited oleic acid access in Amberlyst due to a poor swelling network.[49]

4. CONCLUSIONS

Sustainable routes for granular (GAC) and carbon monolith sulfonation have been developed using the incipient wetness method and sonication with hydrothermal or plasma activation. Significantly lower activating agent to catalyst mass ratios were used to synthesize the materials, yet activity and stability was similar to a commercial catalyst (Amberlyst-15) derived from petroleum resources. For example, 0.62 to 1.75 mL/g was used in this work compared to 7−50 mL/g in the literature[8−10] and TOF's greater than Amberlyst. If all activating agent ends up as waste, an *E*-factor (kg waste/kg product) 11−46× lower than those reported in the literature is estimated (e.g., E = 1.96 for GAC-HT-2M vs E = 91.5).[9] Although the plasma treatments generated lower acid site density and esterification reaction rates (mmol/g-cat/min), the plasma method was validated for synthesis of acid functionalized carbon monoliths. Further improvements in the plasma technique could generate an optimum ratio of strong and weak acid sites that can be scaled more easily to larger sized monoliths, pellets, or granules. The carbon catalysts were also stable; GAC-HT-18M retained 98.9% catalytic activity, comparable to Amberlyst-15, and GAC-HT-2M retained over 85% of its catalytic activity after 4 runs. However, both the sulfonated ACM catalysts showed a decline in E-2HIBA yield and catalytic activity. Because ACM was crushed to use in the agitated batch reactions, attrition (loss of carbon support with $C—SO_3—H^+$ sites) may have contributed to the activity decline; future testing in monolith form is required to confirm this theory. Further plasma optimization, by increasing power and H_2 concentration may generate higher $-C—SO_3^-H^+$

https://doi.org/10.1021/acs.iecr.2c00086
Ind. Eng. Chem. Res. 2022, 61, 3928−3940

densities and results comparable to the hydrothermal treatment. This work provides two sustainable sulfonation methods, both hydrothermal and plasma, for the synthesis of sulfonated carbon catalysts, which may have widespread applications in the synthesis of various esters from biobased organic acids. The acid carbon monolith could provide a more efficient and sustainable platform for continuous esterification processes in fine and specialty chemical industries.

■ ASSOCIATED CONTENT

Supporting Information

The Supporting Information is available free of charge at https://pubs.acs.org/doi/10.1021/acs.iecr.2c00086.

(1) Apparatus for plasma treatment, (2) methods for batch reactions, FTIR and XPS analyses, comparison of plasma treatments, (3) STEM-EDS for base GAC (untreated), (4) STEM-EDS for base cACM (untreated activated carbon monolith), (5) EDS images for fresh and spent GAC and cACM catalysts, (6) FTIR peak assignments, (7) XPS peak assignments, (8) FTIR figures, (9) plot of TOF versus carbon catalyst and strong acid site density (PDF)

■ AUTHOR INFORMATION

Corresponding Author

James R. Kastner − *Riverbend North Research Lab, Biochemical Engineering, College of Engineering, The University of Georgia, Athens, Georgia 30602, United States;* orcid.org/0000-0003-0216-0158; Phone: 706-583-0155; Email: jrk@uga.edu; Fax: 706-542-8806

Author

Sarada Sripada − *Riverbend North Research Lab, Biochemical Engineering, College of Engineering, The University of Georgia, Athens, Georgia 30602, United States*

Complete contact information is available at: https://pubs.acs.org/10.1021/acs.iecr.2c00086

Notes

The authors declare no competing financial interest.

■ ACKNOWLEDGMENTS

Support for this research was provided by the USDA-NIFA Grant (Carbon Monolith Catalysts from Wood for Biobased Platform Chemicals: 2017-67021-26136). The authors thank Myranda Jackson, Applied Catalysts, for her contribution in performing the BET surface area analysis, and Dr. Kun Yao and Seyedehsan Vasefi for assistance with the plasma work. The XPS analysis was performed at the Georgia Tech Institute for Electronics and Nanotechnology or Joint School of Nanoscience and Nanotechnology, a member of the National Nanotechnology Coordinated Infrastructure (NNCI), which is supported by the National Science Foundation (Grant ECCS-1542174).

■ REFERENCES

(1) Wang, C.; Gui, X.; Yun, Z. Esterification of lauric and oleic acids with methanol over oxidized and sulfonated activated carbon catalyst. *Reac. Kinet. Mech. Catal.* **2014**, *113*, 211−223.

(2) Sudarsanam, P.; Zhong, R.; Van den Bosch, S.; Coman, S. M.; Parvulescu, V. I.; Sels, B. F. Functionalized heterogeneous catalysts for sustainable biomass valorization. *Chem. Soc. Rev.* **2018**, *47*, 8349−8402.

(3) Kokel, A.; Schäfer, C.; Török, B. Organic Synthesis Using Environmentally Benign Acid Catalysis. *Curr. Org. Synth.* **2019**, *16*, 615−649.

(4) Lou, W.-Y.; Guo, Q.; Chen, W.-J.; Zong, M.-H.; Wu, H.; Smith, T. J. A highly active bagasse-derived solid acid catalyst with properties suitable for production of biodiesel. *ChemSusChem.* **2012**, *5*, 1533−1541.

(5) Siril, P. F.; Cross, H. E.; Brown, D. R. New polystyrene sulfonic acid resin catalysts with enhanced acidic and catalytic properties. *J. Mol. Catal. A- Chem.* **2008**, *279*, 63−68.

(6) Konwar, L. J.; Maki-Arvela, P.; Mikkola, J.-P. SO_3H- Containing Functional Carbon Materials: Synthesis, Structure, and Acid Catalysis. *Chem. Rev.* **2019**, *119*, 11576−11630.

(7) Kastner, J. R.; Miller, J.; Geller, D. P.; Locklin, J.; Keith, L. H.; Johnson, T. Catalytic esterification of fatty acids using solid acid catalysts generated from biochar and activated carbon. *Catal.* **2012**, *190*, 122−132.

(8) Fraile, J. M.; Garcia-Bordeje, E.; Roldan, L. Deactivation of sulfonated hydrothermal carbons in the presence of alcohols: Evidence for sulfonic esters formation. *J. Catal.* **2012**, *289*, 73−79.

(9) Adhikari, S.; Hood, Z.; Gallego, N.; Contescu, C. Lignin-Derived Carbon Fibers as Efficient Heterogeneous Solid Acid Catalysts for Esterification of Oleic Acid. *MRS Adv.* **2018**, *3*, 2865−2873.

(10) Chong, C. C.; Cheng, Y. W.; Lam, M. K.; Setiabudi, H. D.; Vo, D-V.N. *Energy Technol.* **2021**, *9*, 2100303.

(11) Pang, J.; Wang, A.; Zheng, M.; Zhang, T. Hydrolysis of cellulose into glucose over carbons sulfonated at elevated temperatures. *Chem. Commun.* **2010**, *46*, 6935−6937.

(12) Miao, Y.; Ma, Y.; Wang, Q. Plasma-Assisted Simultaneous Reduction and Nitrogen/Sulfur Codoping of Graphene Oxide for High-Performance Supercapacitors. *ACS Sustainable Chem. Eng.* **2019**, *7*, 7597−7608.

(13) Wang, Z.; Zhang, Y.; Neyts, E. C.; Cao, X.; Zhang, X. W.-L.; Jang, B.; Liu, C.-J. Catalyst Preparation with Plasmas: How does it Work? *ACS Catal.* **2018**, *8*, 2093−2110.

(14) Li, O. L.; Ikura, R.; Ishizaki, T. Hydrolysis of cellulose to glucose over carbon catalysts sulfonated *via* a plasma process in dilute acids. *Green Chem.* **2017**, *19*, 4774−4777.

(15) Qin, L.; Takeuchi, N.; Takahashi, K.; Kang, J.; Kim, K. H.; Li, O. L. N_2/Ar plasma-induced surface sulfonation on graphene nanoplatelets for catalytic hydrolysis of cellulose to glucose. *Appl. Surf. Sci.* **2021**, *545*, 149051.

(16) Horikoshi, S.; Serpone, N. In-liquid plasma: a novel tool in the fabrication of nanomaterials and in the treatment of wastewaters. *RSC Adv.* **2017**, *7*, 47196.

(17) Pirmoradi, M.; Janulaitis, N.; Gulotty, R. J., Jr; Kastner, J. R. Bi-Metal-Supported Activated Carbon Monolith Catalysts for Selective Hydrogenation of Furfural. *Ind. Eng. Chem. Res.* **2020**, *59*, 17748−17761.

(18) Sachse, A.; Galarneau, A.; Coq, B.; Fajula, F. Monolithic flow microreactors improve fine chemical synthesis. *New J. Chem.* **2011**, *35*, 259−264.

(19) Bhalla, T. C.; Kumar, V.; Bhatia, S. K. Hydroxy acids: Production and applications. In *Advances in Industrial Biotechnology*; Singh, R. S., Pandey, A., Larroche, C., Eds.; IK International Publishing House PVT. Ltd.: New Delhi, India, 2014; pp 56−76.

(20) Weakley, G. K.; Kelly, C. E. Method for Producing An Alkyl 3-Hydroxybutyrate. Patent Application. US 20150038734 A1, Feb. 5, 2015.

(21) Trombettoni, V.; Sciosci, D.; Bracciale, M. P.; Campana, F.; Santarelli, M. L.; Marrocchi, A.; Vaccaro, L. Boosting biomass valorisation. Synergistic design of continuous flow reactors and water-tolerant polystyrene acid catalysts for a non-stop production of esters. *Green Chem.* **2018**, *20*, 3222.

(22) Rohwerder, T.; Müller, R. H. Biosynthesis of 2-hydroxyisobutyric acid (2-HIBA) from renewable carbon. *Microb. Cell. Fact.* **2010**, *9*, 13.

(23) Nobuyuki, M.; Takafumi, A.; Hirofumi, H. Process for Producing Methyl α-Hydroxyisobutyrate. Patent Application. US005391813 A, Oct 12, 1993.
(24) Ethyl 2-hydroxyisobutyrate; ChemicalBook, https://www.chemicalbook.com/ChemicalProductProperty_EN_CB8376602.htm, 2017 (accessed November 2021).
(25) Rohde, M.-T.; Tischer, S.; Harms, H.; Rohwerder, T. Production of 2-Hydroxyisobutyric Acid from Methanol by Methylobacterium extorquens AM1 Expressing (R)-3- Hydroxybutyryl Coenzyme A-Isomerizing Enzymes. *Appl. Environ. Microbiol.* **2017**, *83*, 1−16.
(26) Miller, I., Freund, J. E. *Probability and Statistics for Engineers*; Prentice-Hall, Inc.: Englewood Cliffs, NJ, 1985.
(27) Hood, Z. D.; Adhikari, S. P.; Evans, S. F.; Wang, H.; Li, Y.; Naskar, A. K.; Chi, M.; Lachgar, A.; Paranthaman, M. P. Tire-derived carbon for catalytic preparation of biofuels from feedstocks. *Carbon Resour. Convers.* **2018**, *1*, 165−173.
(28) Wang, X.; Liu, R.; Waje, M. M.; Chen, Z.; Yan, Y.; Bozhilov, K. N.; Feng, P. Sulfonated Ordered Mesoporous Carbon as a Stable and Highly Active Protonic Acid Catalyst. *Chem. Mater.* **2007**, *19*, 2395−2397.
(29) Liguori, F.; Barbaro, P.; Said, B.; Galarneau, A.; Dal Santo, V.; Passaglia, E.; Feis, A. Unconventional Pd@Sulfonated Silica Monoliths Catalysts for Selective Partial Hydrogenation Reactions under Continuous Flow. *ChemCatChem.* **2017**, *9*, 3245−3258.
(30) Ormsby, R.; Kastner, J. R.; Miller, J. Hemicellulose hydrolysis using solid acid catalysts generated from biochar. *Catal.* **2012**, *190*, 89−97.
(31) Yakout, S. M.; El-Deen, G. S. Characterization of activated carbon prepared by phosphoric acid activation of olive stones. *Arab. J. Chem.* **2016**, *9*, S1155−S1162.
(32) Mateo, W.; Lei, H.; Villota, E.; Qian, M.; Zhao, Y.; Huo, E.; Zhang, Q.; Lin, X.; Wang, C.; Huang, Z. Synthesis and characterization of sulfonated activated carbon as a catalyst for bio-jet fuel production from biomass and waste plastics. *Bioresour. Technol.* **2020**, *297*, 122411.
(33) Galhardo, T. S.; Simone, N.; Goncalves, M.; Figueiredo, F. C. A.; Mandelli, D.; Carvalho, W. A. Preparation of Sulfonated Carbons from Rice Husk and Their Application in Catalytic Conversion of Glycerol. *ACS Sustainable Chem. Eng.* **2013**, *1*, 1381−1389.
(34) Puziy, A.M.; Poddubnaya, O.I.; Martınez-Alonso, A.; Suarez-Garcıa, F.; Tascon, J.M.D. Characterization of synthetic carbons activated with phosphoric acid. *Appl. Surf. Sci.* **2002**, *200*, 196−202.
(35) Nakhate, A. V.; Yadav, G. D. Synthesis and Characterization of Sulfonated Carbon-Based Graphene Oxide Monolith by Solvothermal Carbonization for Esterification and Unsymmetrical Ether Formation. *ACS Sustainable Chem. Eng.* **2016**, *4*, 1963−1973.
(36) Galindo, H.; Carvajal, Y.; Suib, S. L. Sulfonation of the surface of cordierite monoliths through a novel multi-step wet chemical process. *Micropor. Mesopor. Mater.* **2010**, *135*, 37−44.
(37) Peng, X.; Shen, S.; Wang, C.; Li, T.; Li, Y.; Yuan, S.; Wen, X. Influence of relative proportions of cellulose and lignin on carbon-based solid acid for cellulose hydrolysis. *Mol. Catal.* **2017**, *442*, 133−139.
(38) Liu, Z.; Qi, Y.; Gui, M.; Feng, C.; Wang, X.; Lei, Y. Sulfonated carbon derived from the residue obtained after recovery of essential oil from the leaves of *Cinnamomum longepaniculatum* using Brønsted acid ionic liquid, and its use in the preparation of ellagic acid and gallic acid. *RSC Adv.* **2019**, *9*, 5142−5150.
(39) Hou, H.; Shao, L.; Zhang, Y.; Zou, G.; Chen, J.; Ji, X. Large-Area Carbon Nanosheets Doped with Phosphorus: A High-Performance Anode Material for Sodium-Ion Batteries. *Adv. Sci.* **2017**, *4*, 1600243.
(40) Van Deynse, A.; De Geyter, N.; Leys, C.; Morent, R. Influence of Water Vapor Addition on the Surface Modification of Polyethylene in an Argon Dielectric Barrier Discharge. *Plasma Process. Polym.* **2014**, *11*, 117−125.
(41) Peng, L.; Xu, Z.; Liu, Z.; Wei, Y.; Sun, H.; Li, Z.; Zhao, X.; Gao, C. An iron-based green approach to 1-h production of single-layer graphene oxide. *Nat. Commun.* **2015**, *6*, 5716.
(42) Martirosyan, V. Atomistic simulations of H2 and He plasmas modification of thin-films materials for advanced etch processes. Micro and nanotechnologies/Microelectronics. Ph.D. Thesis, Université Grenoble Alpes, 2017. English. NNT: 2017GREAT101.
(43) Hinde, P.; Demidyuk, V.; Gkelios, A.; Tipton, C. Plasma Catalysis: A Review of the Interdisciplinary Challenges Faced. *Johnson Matthey Technol. Rev.* **2020**, *64*, 138−147.
(44) Zhang, W.; Tao, H.; Zhang, B.; Ren, J.; Lu, G.; Wang, Y. One-pot synthesis of carbonaceous monolith with surface sulfonic groups and its carbonization/ activation. *Carbon* **2011**, *49*, 1811−1820.
(45) García-Mateos, F. J.; Ruiz-Rosas, R.; Rosas, J. M.; Rodríguez-Mirasol, J.; Cordero, T. Phosphorus containing carbon (submicron)-fibers as efficient acid catalysts. *Catal. Today* **2022**, *383*, 308−319.
(46) da Luz Corrãa, A. P.; Bastos, R. R. C.; da Rocha Filho, G. N.; Zamian, J. R.; da Conceicão, L. R. V. Preparation of sulfonated carbon-based catalysts from murmuru kernel shell and their performance in the esterification reaction. *RSC Adv.* **2020**, *10*, 20245−20256.
(47) Chaichana, E.; Wiwatthanodom, W.; Jongsomjit, B. Carbon-Based Catalyst from Pyrolysis of Waste Tire for Catalytic Ethanol Dehydration to Ethylene and Diethyl Ether. *Int.J. Chem. Eng.* **2019**, *2019*, 1−10.
(48) Khudsange, C. R.; Wasewar, K. L. Process intensification of esterification reaction for the production of propyl butyrate by pervaporation. *Resource-Efficient Technologies.* **2017**, *3*, 88−93.
(49) Geng, L.; Wang, Y.; Yu, G.; Zhu, Y. Efficient carbon-based solid acid catalysts for the esterification of oleic acid. *Catal. Commun.* **2011**, *13*, 26−30.

https://doi.org/10.1021/acs.iecr.2c00086
Ind. Eng. Chem. Res. 2022, 61, 3928−3940